The AGE-Breaker ALT-711 Restores High Blood Flow–Dependent Remodeling in Mesenteric Resistance Arteries in a Rat Model of Type 2 Diabetes

Mohamed L. Freidja, Kahena Tarhouni, Bertrand Toutain, Céline Fassot, Laurent Loufrani, and Daniel Henrion

Flow-mediated remodeling of resistance arteries is essential for revascularization in ischemic diseases, but this is impaired in diabetes. We hypothesized that breaking advanced glycation end product (AGE) cross-links could improve remodeling in mesenteric resistance arteries in Zucker diabetic fatty (ZDF) rats compared with lean Zucker (LZ) rats. Arteries, exposed to high (HF) or normal (NF) blood flow after alternate arterial ligation in vivo, were collected after 2 weeks. In LZ rats, HF artery diameter was larger than for NF vessels, but this was not the case in ZDF rats. Endothelium-mediated dilation in ZDF rats, which was lower than in LZ rats, was further decreased in HF arteries. Treatment of rats with the AGE-breaker 4,5-dimethyl-3-phenacylthiazolium chloride (ALT-711) (3 mg/kg/day; 3 weeks) reversed diabetes-induced impairment of HF-dependent remodeling. ALT-711 also improved endothelium nitric oxide–dependent relaxation in mesenteric resistance arteries. Reactive oxygen species reduction restored relaxation in ZDF rats but not in LZ or ALT-711–treated rats. AGEs were reduced in ALT-711–treated ZDF rats compared with ZDF rats. Metalloproteinase activity, necessary for HF-dependent remodeling, was reduced in ZDF rats compared with LZ rats and restored by ALT-711. Thus, targeting AGE cross-links may provide a therapeutic potential for overcoming microvascular complications in ischemic disorders occurring in diabetes. ***Diabetes*** **61:1562–1572, 2012**

Type 2 diabetes is the most frequently encountered metabolic disorder, currently affecting 5–10% of the population (1). Associated with obesity, type 2 diabetes is characterized by insulin resistance, inducing several metabolic changes, including hyperinsulinemia, hyperglycemia, dyslipidemia, and hypertension, all of which lead to an increased risk of cardiovascular events (2). The morbidity and mortality associated with type 2 diabetes essentially are related to vascular lesions that develop over time with this condition (3). Microcirculation primarily is involved, and therefore vital organs are damaged. Although the consequences of type 2 diabetes on large elastic arteries have been extensively studied (4,5), less is known about its effects on microcirculation. Nevertheless, we have previously shown that the ability of resistance arteries to adapt their structure and function in response to a chronic rise in blood flow is impaired in Zucker diabetic fatty (ZDF) rats (6).

The primary function of microcirculation is to optimize nutrient and oxygen supply within tissues in response to metabolic demand. For this purpose, resistance arteries can adapt to chronic increases in blood flow, leading to diameter enlargement (outward remodeling) and higher endothelium nitric oxide (NO)-dependent relaxation (7–9). This remodeling is involved as a response to an increase in the metabolic demand of different tissues during growth, following exercise training, or during pregnancy (10). The production of NO by the endothelium and the activation of matrix metalloproteinases (MMPs) are required for flow-mediated remodeling of small resistance (9) and large elastic arteries (11). In conditions involving a reduced endothelial ability to produce vasodilator agents, such as aging, increasing chronically local blood flow has been shown to improve endothelium NO–dependent dilation. This was associated with reduced reactive oxygen species (ROS) production and improved endothelial NO synthase (eNOS) protein expression and activation (12).

Type 2 diabetes is associated with an increase in ROS production (13) that might impair the ability of resistance arteries to adapt their structure and function in response to chronic increases in blood flow attributed to decreased NO bioavailability (14). Nevertheless, because both ROS and NO also are required for flow-mediated remodeling (15), the effect of ROS overproduction on remodeling cannot be deduced from previous studies. In fact, our previous work performed on obese Zucker rats has shown that flow-induced remodeling (diameter enlargement) occurred in spite of obesity and slight hypertension and hyperglycemia. In ZDF rats, we found that flow-mediated diameter enlargement and the associated compensatory media hypertrophy did not occur in combination with a further reduction in endothelium-mediated dilation (6). Because the response to flow was globally altered, we hypothesized that advanced glycation end products (AGEs) might be involved in this dysfunction observed in type 2 diabetic rats. AGEs are generated by nonenzymatic glycation of structural proteins by glucose. This process accompanies normal aging and occurs at an accelerated rate in diabetes (16,17).

To verify this hypothesis, we used a model of ligature of the mesenteric arterial bed (18–20), allowing us to compare resistance arteries chronically submitted to high (HF) or normal (NF) blood flow levels, under the same physiological conditions. We used ZDF rats that either were treated with the AGE-breaker 4,5-dimethyl-3-phenacylthiazolium chloride (ALT-711) or left untreated, hypothesizing that coupling the chronic rise in blood flow to a reduction in the AGE level would improve the ability of resistance arteries to respond to chronic changes in blood flow.

From the Department of Integrated Neurovascular Biology, INSERM U771, Centre National de la Recherche Scientifique UMR 6214, Université d'Angers, Angers, France.
Corresponding author: Daniel Henrion, daniel.henrion@univ-angers.fr.
Received 31 May 2011 and accepted 8 February 2012.
DOI: 10.2337/db11-0750
This article contains Supplementary Data online at http://diabetes.diabetesjournals.org/lookup/suppl/doi:10.2337/db11-0750/-/DC1.
M.L.F. and K.T. contributed equally to this work.

RESEARCH DESIGN AND METHODS

Twenty adult male ZDF and 20 lean Zucker (LZ) rats, 11–12 weeks old, were purchased from Charles River (L'Arbresles, France). They were anesthetized (isoflurane, 2.5%) and submitted to surgery to modify blood flow, as previously described (19,21,22). In brief, three consecutive first-order mesenteric arteries were used. Ligatures (7–0 silk surgical thread) were applied to second-order branches of the first and third arteries, as shown in Fig. 1*A*. The artery located between two ligated arteries was designated as an HF artery. Other arteries located further from the ligated arteries were used as control (NF) arteries. Rats were treated with buprenorphine (0.1 mg/kg s.c. temgesic) before and after surgery. One-half of the rats were treated by intraperitoneal injection with ALT-711 (3 mg/kg/day). Treatment started 1 week before surgery. Consequently, the total duration of the treatment was 3 weeks.

Fourteen days after surgery, the animals were anesthetized (isoflurane, 2.5%). The right femoral artery was catheterized for blood pressure measurement (23). The animals then were killed by CO_2 inhalation, the gut excised, and the mesenteric arteries gently dissected. HF and NF arteries from each rat were isolated and divided into several segments used respectively for pressure-diameter relationship measurement, pharmacology, biochemistry, and immunohistological analyses. Before the animals were killed, glycemia was quantified on a sample of arterial blood with a glucometer (9).

The procedure followed in caring for and killing the study animals complied with the European Community Standards on the Care and Use of Laboratory Animals (authorization no. 6422; Ministère de l'Agriculture, France) and the Principles of Laboratory Animal Care (NIH publication no. 85–23, revised 1985; available at http://grants1.nih.gov/grants/olaw/references/phspol.htm). The protocol was approved by the regional ethics committee (protocol CEEA PdL 2008.10).

Pressure-diameter relationship and in vitro cross-sectional compliance in HF and NF arteries. Segments of NF and HF arteries were cannulated at both ends and mounted on a video-monitored perfusion system (24). Arterial segments were perfused and superfused with a Ca^{2+}-free physiological salt solution (PSS) containing EGTA (2 mmol/L) and sodium nitroprusside (SNP) (10 μmol/L) and submitted to a stepwise increase in pressure (10–150 mmHg) in order to determine arterial passive diameter. Data were recorded using a Biopac data acquisition system (La Jolla, CA) and analyzed (Acqknowledge software). Arterial compliance was calculated as previously described (25). In short, during the stepwise increase in pressure (10–150 mmHg), the cross-sectional compliance (CSC) of mesenteric resistance arteries was calculated by the ratio of lumen area (ΔA) and pressure (ΔP) as CSC = ΔA/ΔP.

Pharmacological profile of isolated HF and NF arteries. Other segments of HF and NF mesenteric arteries (2 mm long) were dissected and mounted on a wire myograph (DMT, Aarhus, DK) (26). Two tungsten wires (25 μm in diameter) were inserted into the lumen of the arteries and fixed to a force transducer and a micrometer, respectively. Arteries were bathed in a PSS. Wall tension was applied as previously described (27). The artery's viability was tested using a potassium-rich solution (KCl, 80 mmol/L). A cumulative concentration-response curve (CRC) to acetylcholine (ACh; 0.001 to 10 μmol/L) was performed after a precontraction induced by phenylephrine to ~50% of the maximal response. Then, a CRC to 5-hydroxy-tryptamine (0.001–10 μmol/L) was completed. Thirty minutes after washout, a second CRC to ACh (0.001–10 μmol/L) was performed in the presence of L-NG-nitro-L-arginine methyl ester (L-NAME) (100 μmol/L) or in the presence of superoxide dismutase (120 units/mL) plus catalase (80 units/mL). Finally, a CRC to SNP (0.001–10 μmol/L) was performed. In another series of experiments, a CRC to L-NAME (0.01–100 μmol/L) was performed after a precontraction induced by phenylephrine to ~10% of the maximal response.

Western blot analysis. The remaining NF and HF arteries of each mesenteric vascular bed were pooled and then homogenized. Proteins (25 μg total protein from each sample) were separated by SDS-PAGE using a 4% stacking gel, followed by a 10% running gel. Proteins were detected with specific antibodies (eNOS 1:1,000, phospho-eNOS 1:500, AGE 1:100, receptor for advanced end products [RAGE] 1:500, and β-actin 1:1,000 in bovine serum albumin in Tris-buffered saline with Tween [T-TBS-BSA] 5%; Transduction Laboratories). Protein expression was visualized using the ECL Plus chemiluminescence kit (Amersham) (28).

Immunohistological analysis. As previously described (24), segments of mesenteric resistance arteries were mounted in embedding medium (Tissu-Tek; Miles), frozen in isopentane precooled in liquid nitrogen, and stored at −80°C. Transverse cross-sections (7 μm thick) were used for cyclooxygenase (COX)-2 (24), advanced end products (AGEs) (29), and methylglyoxal-derived hydroimidazolene (MG-^{1}H) (30). Fluorescence staining was visualized using confocal microscopy and image analysis (Histolab; Microvision, Paris, France) (9).

In situ zymography. MMP activity was determined by in situ zymography, as previously described (31). Arterial segments isolated from LZ or ZDF rats were incubated for 15 min with angiotensin II (100 nmol/L) in PSS. Arteries then were quickly embedded vertically in Tissue-Tek and frozen. Frozen sections (7 μm thick) were incubated overnight (37°C) with a fluorogenic gelatin substrate (Molecular Probes) dissolved to 25 μg/mL in zymography buffer (50 mmol/L Tris-HCl, 10 mmol/L $CaCl_2$, and protease inhibitor cocktail, pH 7.4). The gelatin with a fluorescent tag remains caged until the gelatin is cleaved by gelatinase activity. In situ gelatinolysis was revealed by the appearance of fluorescence visualized and quantified using confocal microscopy. In control experiments, sections were incubated with MMP inhibitors (1,10-phenanthroline or EDTA).

Histology. Segments of mesenteric arteries were bathed in Ca^{2+}-free PSS containing 10 μmol/L SNP. Pressure was set at 75 mmHg, and the artery was fixed in a 10% buffered formaldehyde solution, as previously described (32). Sections (7 μm thick) were stained with orcein. External diameter, lumen diameter, and media thickness were determined after image acquisition (Olympus T100 microscope, Sony camera) and analyzed using Histolab software (Microvision) for cross-sectional area calculation, as previously described (6).

Statistical analysis. Results were expressed as a means ± SEM. Significance of the variances between groups was determined by a two-way ANOVA for repeated measurements, in pressure-diameter or CRCs. For the other experiments, we used a one-way ANOVA, followed by the Bonferroni post hoc test or a *t* test. Values of $P < 0.05$ or lower were considered to be statistically significant.

RESULTS

Physiological parameters. Rat body weight was slightly, but not significantly, higher in ZDF rats than in LZ rats (363 ± 17 g vs. 336 ± 21 g; $P < 0.05$) and was not significantly affected by ongoing treatment with ALT-711 in either ZDF (353 ± 10 g) or LZ (347 ± 19 g) rats. Blood glucose was significantly enhanced in ZDF rats compared with LZ rats (432 ± 55 mg/dL vs. 157 ± 18 mg/dL). Blood glucose was not modified by continued treatment with ALT-711 in either ZDF (447 ± 32 mg/dL) or LZ (166 ± 15 mg/dL) rats. Type 2 diabetes significantly increased mean blood pressure (92 ± 3 mmHg in ZDF vs. 80 ± 3 mmHg in LZ rats; $P < 0.05$). However, mean blood pressure was not affected by ongoing treatment with ALT-711, in either the ZDF (97 ± 4 mmHg) or LZ (83 ± 3 mmHg) rats.

Arterial diameter and structure. In LZ rats, HF artery diameter was significantly larger than in NF arteries (Fig. 1*A*). In contrast, HF artery diameter in ZDF rats did not increase significantly compared with NF arteries (Fig. 1*B*). Thus, arterial outward remodeling did not occur in ZDF rats. In LZ rats treated with ALT-711, remodeling was similar to that in control rats (Fig. 1*C* and *E*). However, in ZDF rats, ALT-711 restored HF-induced remodeling (Fig. 1*D* and *F*) without changing arterial diameter in mesenteric arteries submitted to NF, compared with control rats.

In ZDF rats, in vitro CSC was significantly lower in both HF and NF arteries, compared with LZ animals. The change in vessel CSC during the stepwise increase of intraluminal pressure from 10 to 50 mmHg was greater in the ZDF group of ALT-711–treated animals, whereas changes in CSC in the ALT-711–treated LZ group showed no difference. Hence, the CSC of the mesenteric resistance arteries was significantly increased with the AGE-breaker treatment (Fig. 2*A* and *B*).

Chronic increase in blood flow significantly increased the media cross-sectional area of HF arteries in LZ rats. No difference in media cross-sectional areas was observed between HF and NF arteries from ZDF rats. Nevertheless, type 2 diabetes induced an increase in the media cross-sectional area of the NF artery, compared with LZ rats. The treatment with ALT-771 significantly decreased the media cross-sectional area of NF arteries in ZDF rats (Fig. 2*C*).

Endothelium-dependent relaxation. In both HF and NF arteries from ZDF rats, ACh-induced relaxation was lower than in LZ animals. In rats treated with ALT-711, ACh-induced

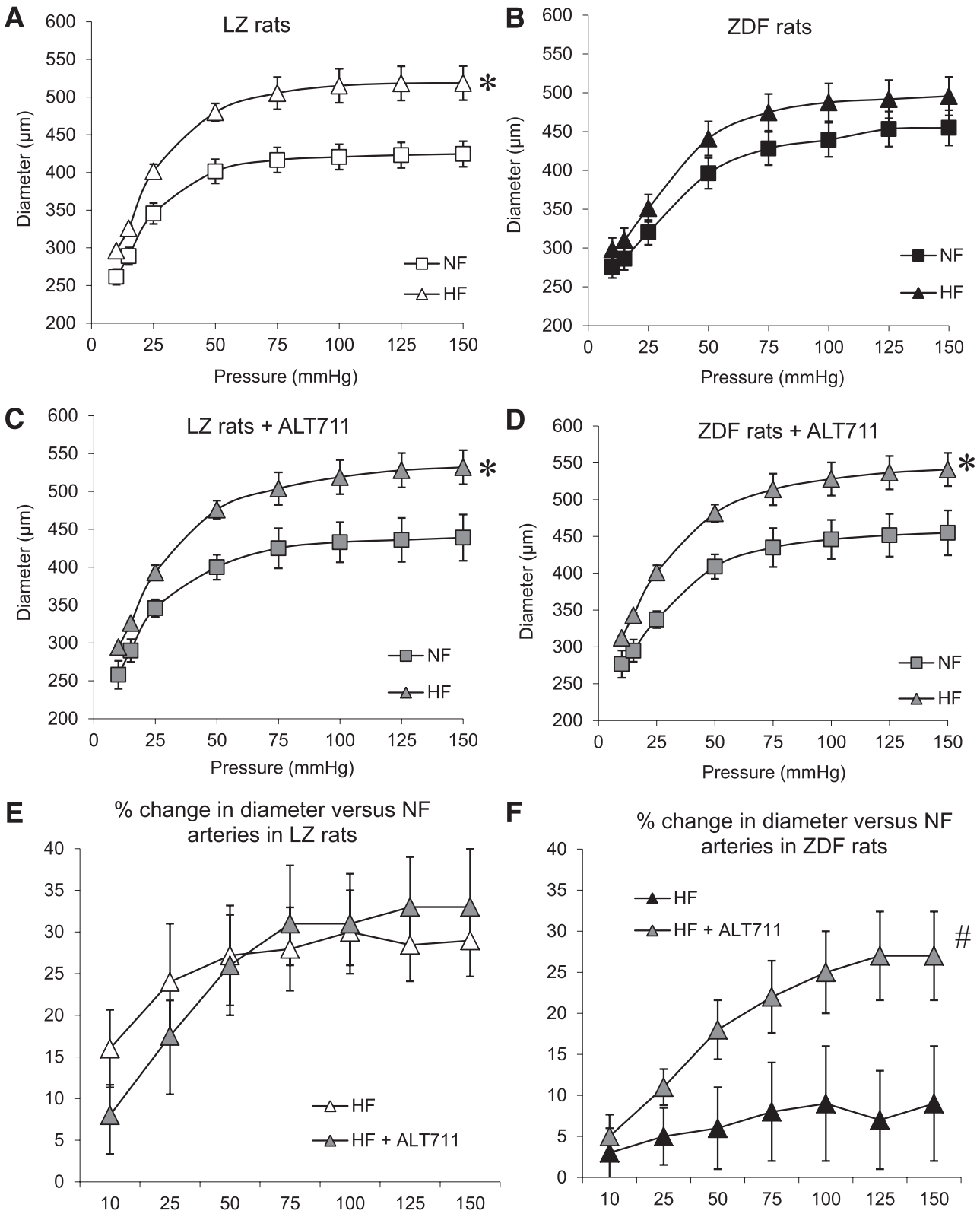

FIG. 1. Changes in diameter in response to stepwise increases in pressure in HF and NF mesenteric resistance arteries isolated from LZ and ZDF rats, either left untreated (*A* and *B*) or treated (*C* and *D*) with the AGE-breaker ALT-711. *E* and *F*: Changes in arterial diameter in HF arteries compared with NF vessels are represented as a percentage of change in diameter. Means ± SEM are presented (n = 10 per group). *$P < 0.05$, HF vs. NF arteries. #$P < 0.05$, ALT-711 vs. control (untreated).

relaxation in HF and NF arteries was improved compared with corresponding arteries from untreated rats (Fig. 3*A* and *C*).

To determine the role of NO in endothelium-dependent dilation, CRCs to ACh were performed in the presence of the NOS inhibitor, L-NAME. In LZ rats, L-NAME abolished ACh-induced relaxation in HF and NF arteries. However in ZDF rats, inhibition of ACh-dependent relaxation with L-NAME was greater under ALT-711 treatment in both NF

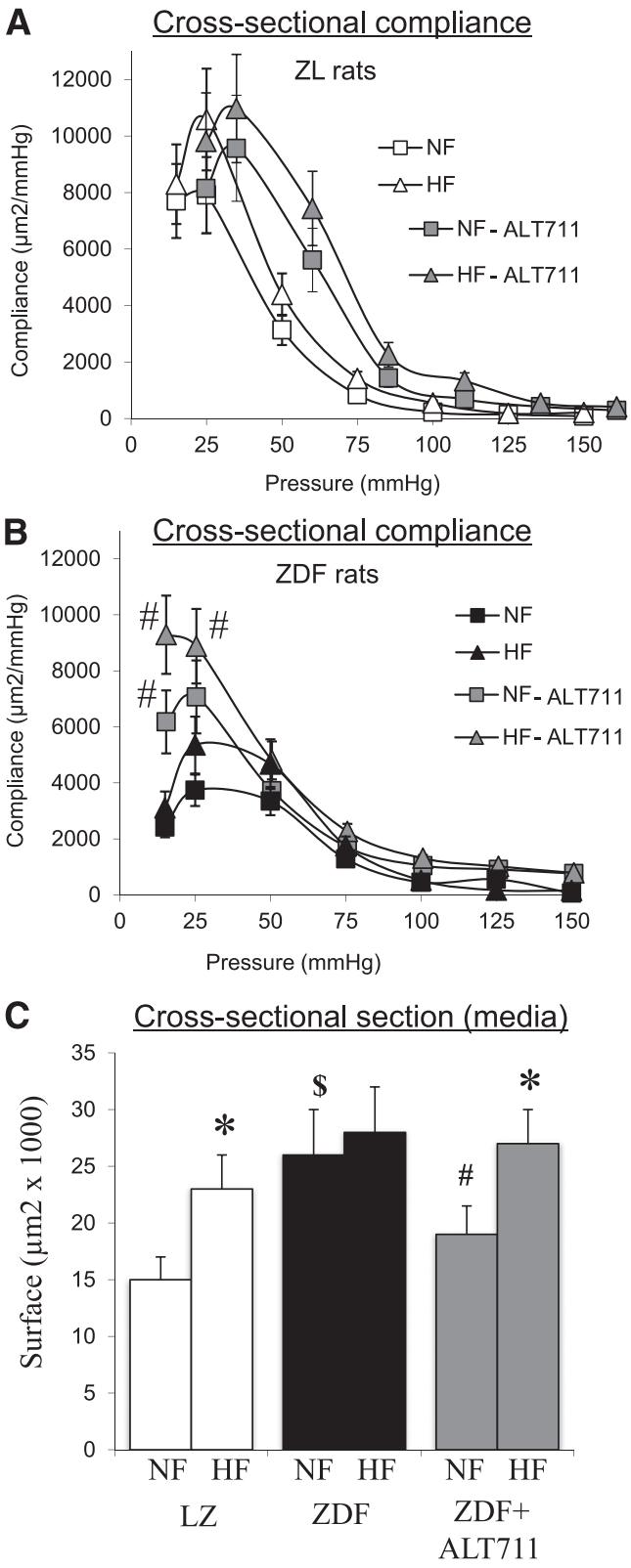

FIG. 2. In vitro cross-sectional compliance determined in response to stepwise increases in pressure from 10 to 150 mmHg in HF and NF mesenteric resistance arteries isolated from LZ (*A*) and ZDF (*B*) rats, either treated with the AGE-breaker ALT-711 or left untreated. *C*: Cross-sectional area of the media. Means ± SEM are presented (n = 10 per group). #$P < 0.05$, ALT-711 vs. control (untreated); *$P < 0.05$, HF vs. NF arteries; \$$P < 0.05$, ZDF vs. LZ.

and HF arteries when compared with vessels from untreated animals (Fig. 3*B* and *D*). The further addition of cyclooxygenase inhibitor indomethacin did not significantly affect dilation (data not shown).

L-NAME–mediated contraction was significantly lower in arteries (NF and HF) from ZDF than from LZ rats, and L-NAME–mediated contraction was higher in ZDF rats treated with ALT-711 than in nontreated rats (Fig. 3*E* and *F*).

The association of SOD plus catalase improved ACh-mediated dilation in both NF and HF arteries from ZDF rats, whereas it did not affect the dilation in arteries isolated from LZ or ZDF rats treated with ALT-711 (Fig. 4). Serotonin (5-hydroxy-tryptamine)-induced contraction and SNP-induced relaxation were not affected by chronic changes in blood flow, by type 2 diabetes or by ALT-711 treatment (Fig. 5).

eNOS protein expression levels. As previously shown by our group (9), eNOS expression levels increased in HF arteries compared with NF vessels in LZ rats (Supplementary Fig. 1). Endothelium dysfunction in ZDF rats was associated with a decreased eNOS expression in HF and NF arteries compared with LZ animals. Of interest, ALT-711 significantly increased eNOS expression in arteries from ZDF rats. Nevertheless, this change in eNOS expression may not totally explain the changes in NO-dependent dilation as ACh-mediated phosphorylation of eNOS increased in both LZ and ZDF rats, treated or not with ALT-711 (Supplementary Fig. 2).

AGE protein expression levels. Mesenteric resistance arteries revealed an increase of AGE formation and RAGE expression in ZDF rats compared with LZ rats. ALT-711 significantly reduced AGE formation and RAGE expression in both HF and NF arteries from diabetic rats (Supplementary Fig. 1). Immunolocalization of AGEs showed the presence of AGEs and MG-^{1}H in mesenteric arteries from ZDF rats and a reduction in AGEs and MG-^{1}H level in ALT-711–treated rats (Fig. 6). Nevertheless, ALT-711 reduced AGE and MG-^{1}H levels in ZDF rats without normalizing their level.

MMP activation. Because MMP activation plays a key role in high flow–mediated remodeling (31), we measured MMP activity (33) in mesenteric arteries (Fig. 7). In arteries from LZ rats, angiotensin II significantly increased MMP activity as assessed by an in situ zymographic gelatinase activity assay. On the other hand, in ZDF rats, angiotensin II induced no significant increase in MMP activity, whereas in ALT-711–treated ZDF rats, angiotensin II significantly increased MMP activity (Fig. 7).

DISCUSSION

In the current study, we found that type 2 diabetes impaired the ability of mesenteric arteries to remodel and improve NO-dependent dilation in response to a chronic increase in blood flow. Indeed, AGEs and RAGEs were overexpressed, whereas eNOS level and MMP activity were reduced in arteries from ZDF rats. Ongoing treatment with the AGE-breaker ALT-711 restored the ability of mesenteric arteries from ZDF rats to increase their diameter and improved endothelium-dependent dilation in response to a chronic rise in blood flow.

Physiologically, a chronic rise in blood flow in resistance arteries enlarges vascular diameter and improves endothelium-dependent dilation (9,19,34). This remodeling is essential to adjust organ perfusion during physiological processes, such as development (35), pregnancy (36), or exercise training

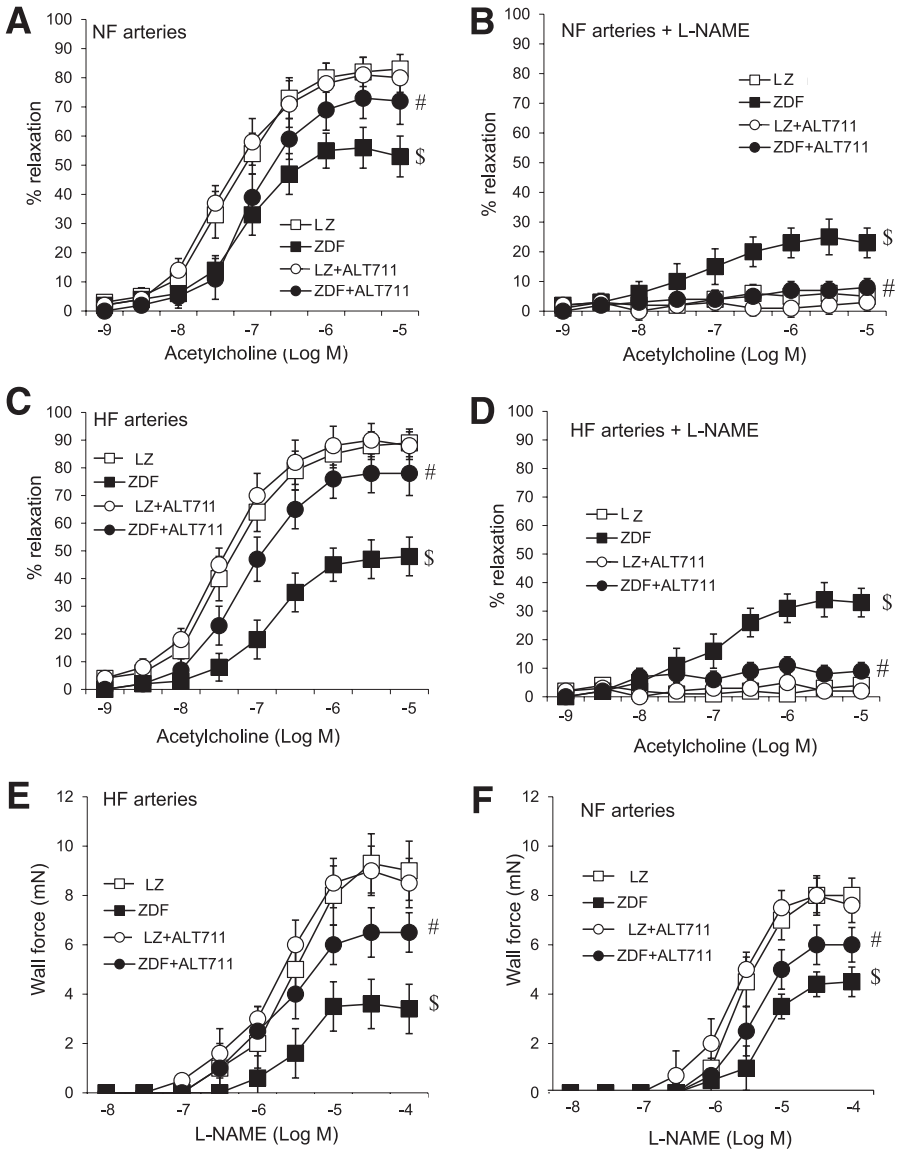

FIG. 3. *A* and *C*: ACh-induced relaxation in HF and NF mesenteric resistance arteries isolated from LZ and ZDF rats. *B* and *D*: Effects of NOS inhibition (L-NAME, 100 μmol/L) on ACh-induced relaxation in HF and NF mesenteric resistance arteries isolated from LZ and ZDF rats. *E* and *F*: L-NAME–mediated contraction in HF and NF mesenteric resistance arteries isolated from LZ and ZDF rats treated or not with ALT-711. $$P < 0.05$, ZDF vs. LZ; #$P < 0.05$, ALT-711 vs. control (untreated).

(37), as well as during pathological processes (mainly ischemic diseases). A similar remodeling also occurs in response to vasodilator treatments (38,39). This remodeling plays a key role in revascularization after occlusion of a large artery, in addition to arteriogenesis and angiogenesis (40). The advantage of the model used in the current study is that it involved resistance arteries and allowed the study of the effects of blood flow on the arterial diameter and wall thickness, independent of blood pressure or metabolic changes and without ischemia.

In type 2 diabetes, the endothelium is less capable of inducing vasodilatation, especially in resistance arteries, which control blood supply to end organs (41). To improve endothelium-dependent dilation, and consequently local blood flow, vasodilator treatments, therapies improving insulin sensitivity, and exercise are commonly used. These treatments are associated with a higher eNOS expression, which is at least partly the consequence of a chronic rise in blood flow (9,34). Here, we show that despite no change in blood glucose level, ALT-711 increased eNOS protein expression in HF and NF arteries from ZDF rats (Fig. 5*A*). Nevertheless, this may not necessarily explain the improvement in ACh-dependent relaxation observed in mesenteric resistance arteries (Fig. 3*A* and *C*) because ACh-mediated phosphorylation of eNOS was equivalent in the different experimental groups. It is most likely that an excessive ROS production reduces NO bioavailablity in arteries of ZDF rats and consequently endothelium-mediated relaxation. Indeed, both inflammation, evidenced by an increased MCP-1, CD68, COX-2, and inducible NOS expression mRNA level (Supplementary Fig. 3) and ROS production, evidenced by a higher 3-nitrotyrosine expression (Supplementary Fig. 4), were higher in arteries from ZDF rats, compared with LZ rats. An immunohistological detection of inducible NOS and COX-2 confirmed the occurrence of inflammation in ZDF rat arteries (Supplementary Figs. 5

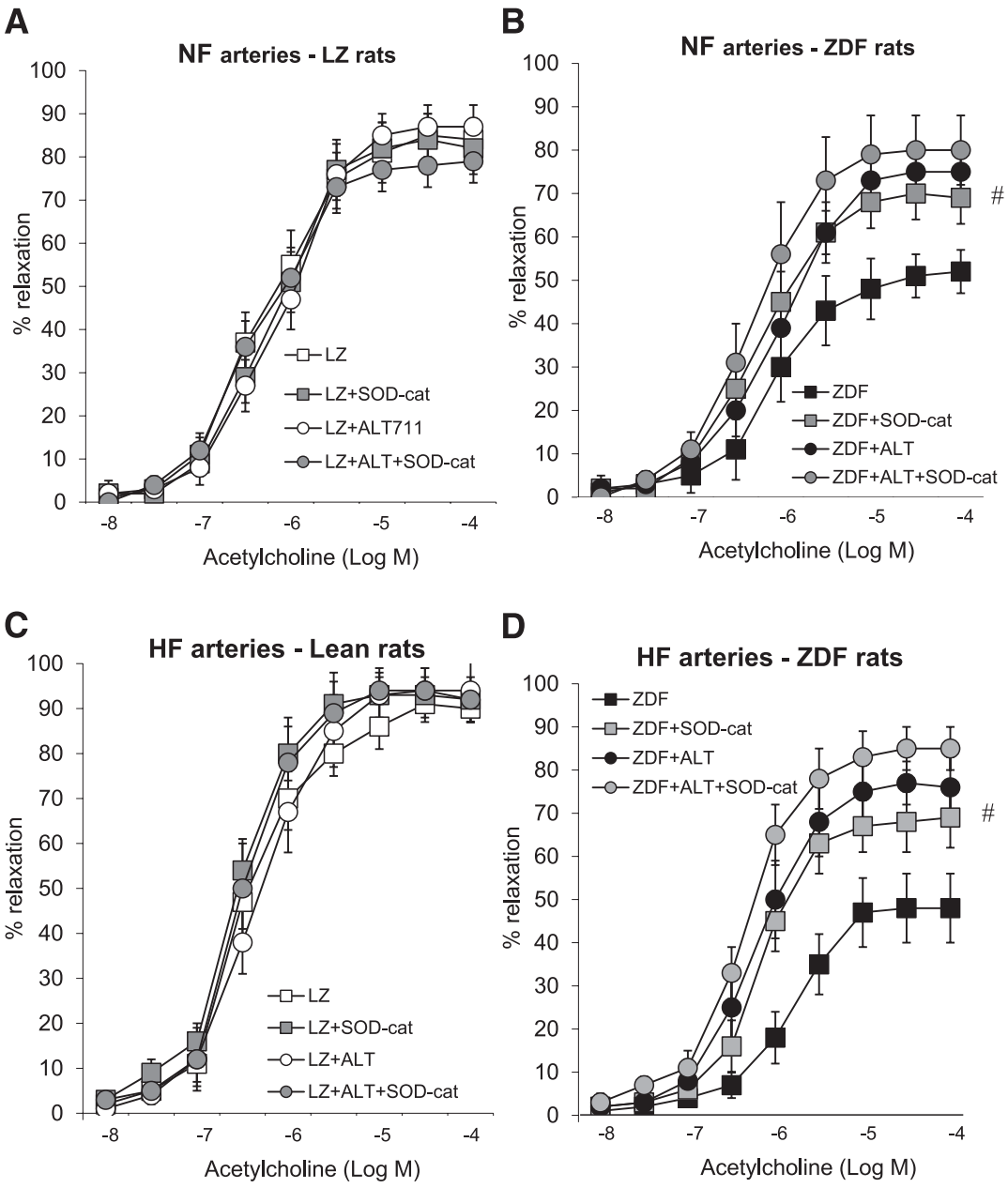

FIG. 4. Effect of SOD and catalase (SOD-cat) on ACh-induced relaxation in NF (*A* and *B*) and HF (*D* and *E*) mesenteric resistance arteries isolated from LZ (*A* and *C*) and ZDF (*B* and *D*) rats. #$P < 0.05$, ALT-711 vs. control (untreated).

and 6). A treatment with ALT-711 reduced both inflammation and oxidative stress.

Our findings are in agreement with a work performed by Su et al. (17), providing a link between AGE formation, oxidative stress, and resistance artery endothelial dysfunction in type 2 diabetic mice. In addition, we have previously shown that the effect of a chronic rise in blood flow on vascular function and remodeling in resistance arteries in type 2 diabetes is impaired and associated with excessive ROS production. However, ROS reduction with catalase and superoxide dismutase (present study) or with tempol (6) restored endothelium-mediated relaxation. On the other hand, a chronic treatment with tempol (6) did not fully restore flow-mediated remodeling or diameter enlargement (6) compared with ALT-711 (present study). As a result, besides superoxide production affecting the endothelium, another mechanism prevents diameter enlargement because antioxidant treatment did not restore flow-mediated remodeling despite a reduction in superoxide level (6).

A possible explanation for the altered HF-dependent remodeling in ZDF rats is that type 2 diabetes already has induced an outward hypertrophic remodeling (42–45) and that a further increase in diameter is no longer possible. Nevertheless, after chronic treatment with ALT-711, an increase in diameter was observed and found to be equivalent to that in LZ rats. The initial flow-sensing process was probably not affected in ZDF rats, because the response to the chronic rise in flow was "normal" with a rise in media cross-sectional area in HF arteries equivalent to that observed in LZ rats. Thus, the reduction in HF-induced diameter enlargement might be caused by the presence of AGEs, which have been shown to reduce the activity of several processes

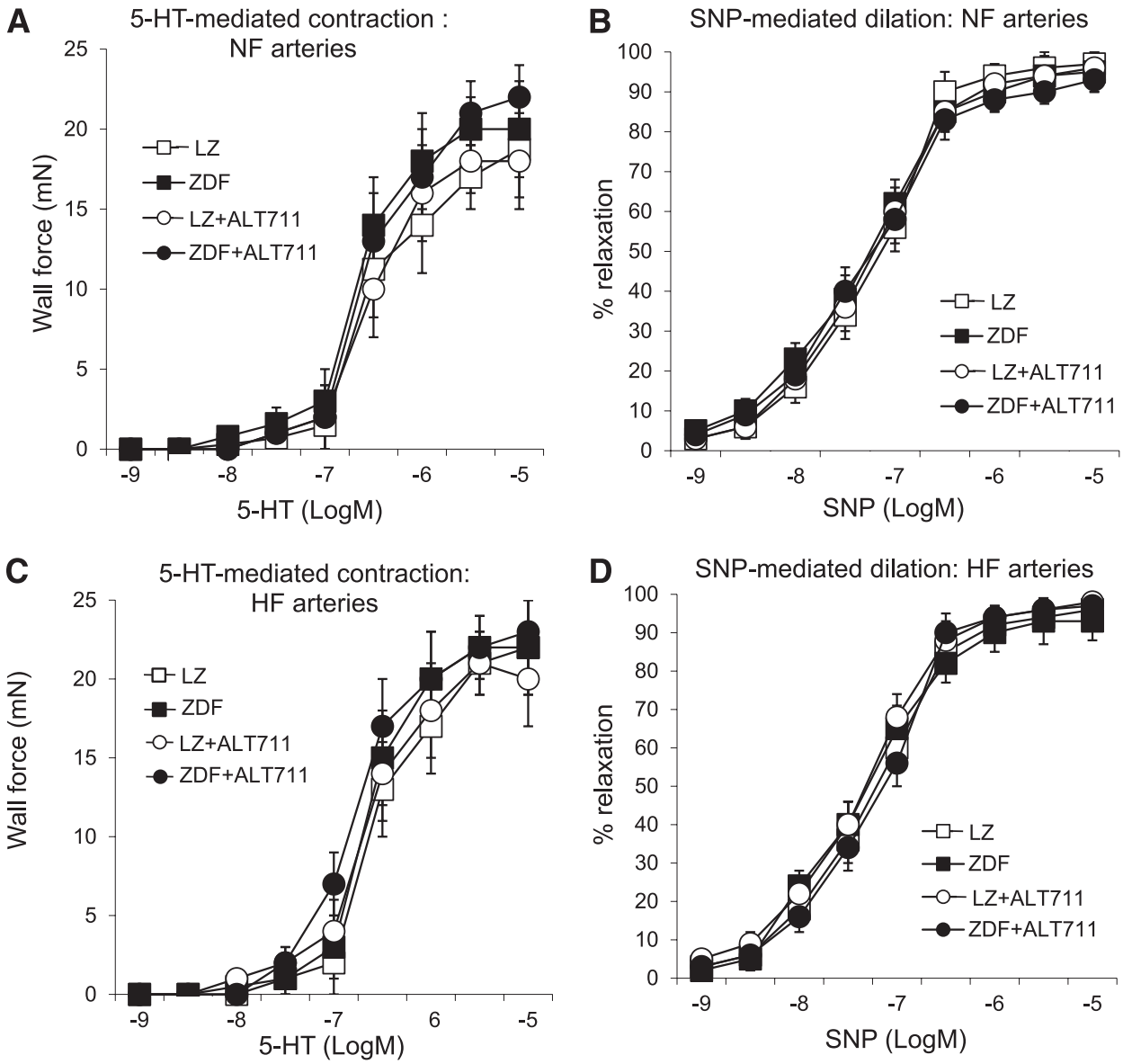

FIG. 5. Cumulative CRCs to serotonin (5-hydroxy-tryptamine [5-HT]) (*A* and *C*) and SNP (*B* and *D*) obtained in mesenteric resistance arteries submitted to a chronic increase in blood flow for 2 weeks (HF arteries), compared with control arteries exposed to NF. Arteries were isolated from LZ and ZDF rats, either treated with ALT-711 or left untreated. Means ± SEM are presented (n = 10 per group).

in type 2 diabetes. AGEs have been reported to alter the matrix proteins collagen, vitronectin, and laminin through AGE-AGE intermolecular covalent bonds or cross-linking (45,46). Furthermore, AGE cross-linking on type I collagen and elastin causes an increase in the extracellular matrix area, resulting in increased stiffness of the vasculature (46). The most probable explanation for this defect is that MMP activity is reduced in arteries from ZDF rats, as evidenced by our experiments (Fig. 7). Indeed, in situ gelatinase activity was reduced in ZDF rats and increased by ALT-711. This effect was most probably mediated by restoration of matrix degradation processes, which are reduced as a result of AGE accumulation. This is in agreement with a previous study showing that preventing AGE formation in streptozotocin-induced diabetic mice restored MMP activity and post-occlusion revascularization (29).

We also found that endothelium-dependent dilation was not improved but instead was further reduced in arteries from ZDF rats submitted to a chronic rise in blood flow, in agreement with our previous work (6). Furthermore, HF arteries from ZDF rats exhibited a greater reduction in endothelium-dependent dilation than NF arteries from ZDF rats (Fig. 3*A* and *C*), showing that a further endothelial dysfunction occurred in response to the chronic increase in blood flow. The defect observed in ZDF rats was not a result of a change in smooth muscle response to NO, because the relaxation induced by the NO donor SNP was not affected. On the other hand, the involvement of NO in the dilation was severely reduced, as evidenced by the reduction of L-NAME's effect on ACh-induced relaxation. In LZ rats, L-NAME strongly reduced ACh-induced relaxation, in agreement with previous studies showing the key role of NO in the mesenteric arteries (9,12). Of interest, in ZDF rats ALT-711 significantly improved NO-dependent relaxation in both NF and HF vessels (Fig. 3). This lower capacity of NO to induce relaxation also was evidenced by a reduced ability of L-NAME

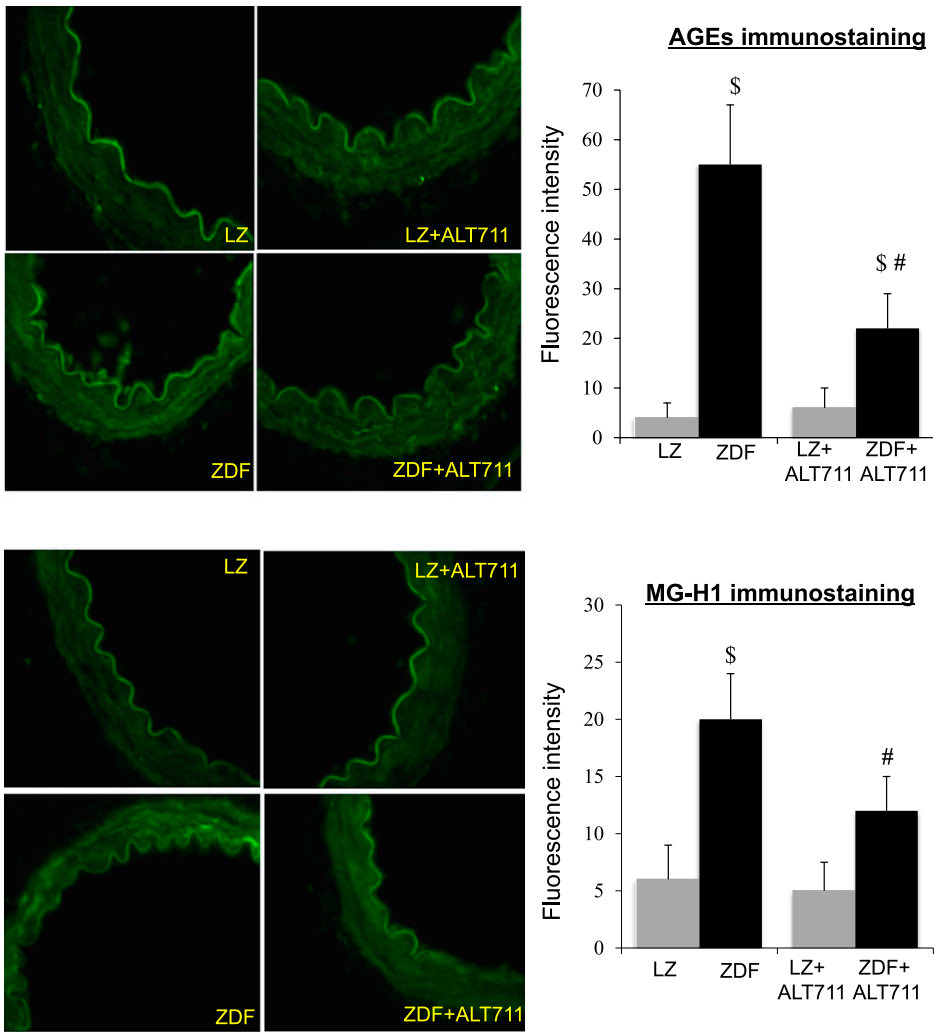

FIG. 6. Immunohistological detection of AGEs and MG-^{1}H in HF and NF mesenteric resistance arteries isolated from ZDF or LZ rats. Values are presented as means ± SEM, n = 8 per group. #P < 0.05, ALT-711 vs. control (untreated); \$$P$ < 0.05, ZDF vs. LZ. (A high-quality color representation of this figure is available in the online issue.)

to induce contraction following precontraction (Fig. 3*E* and *F*). These findings agree with previous studies showing a deleterious effect of AGEs on endothelium-dependent dilation (17,47), although our study provides direct evidence that AGE breaking might reverse vascular damage, especially in response to a chronic increase in blood flow. The reduction in NO-dependent dilation is probably the result of a reduced NO bioavailability, as suggested by two experiments: *1*) the ratio of phospho-eNOS to eNOS, reflecting eNOS activity, was not different in ZDF rats, LZ rats, and ZDF rats treated with ALT-711 (Supplementary Fig. 2) and *2*) ROS reduction with superoxide dismutase and catalase restored ACh-dependent dilation in ZDF rats to the level found in LZ rats (Fig. 4).

Thus, AGEs not only block diameter enlargement in response to a chronic rise in blood flow, they also increase the endothelial dysfunction already present in ZDF rats. We can draw multiple conclusions from the current study. First, increasing flow, which is expected to increase arterial diameter and improve endothelium-dependent dilation, is not only inefficient in ZDF rats but it accelerates endothelial dysfunction. This finding might be of importance when recommending exercise or prescribing vasodilators to diabetic patients. Indeed, both aim to induce flow-mediated outward remodeling (38,48). However, breaking AGEs not only improved endothelial function, but our study suggests that it also might improve local blood flow supply and hence prevent damage to end organs. Thus, breaking AGEs and/or preventing their formation certainly is an important way of reducing ischemic disorders associated with diabetes.

Nevertheless, because ALT-711 also reduced early AGEs such as MG-^{1}H, we cannot exclude that ALT-711 also could reduce AGE formation, at least in part. Furthermore, some beneficial effects of ALT-711, such as improved endothelium-dependent dilation, might result, at least in part, from reduced RAGE stimulation. This is suggested by our results showing that ALT-711 reduced inflammation and oxidative stress in arteries of ZDF rats. Thus, a more in-depth analysis of the effect of AGEs, per se, and of those of RAGE would be necessary in the remodeling process.

In summary, AGE formation in type 2 diabetes altered the ability of resistance arteries to adapt their structure and function in response to a chronic increase in blood flow (summary of the main results of the study in Fig. 8). This impairment was reversed by an AGE-breaking treatment that reduced both AGE level and RAGE expression. Thus, breaking AGE cross-links provides a therapeutic potential for overcoming the microvascular complications of ischemic diseases in long-term diabetes.

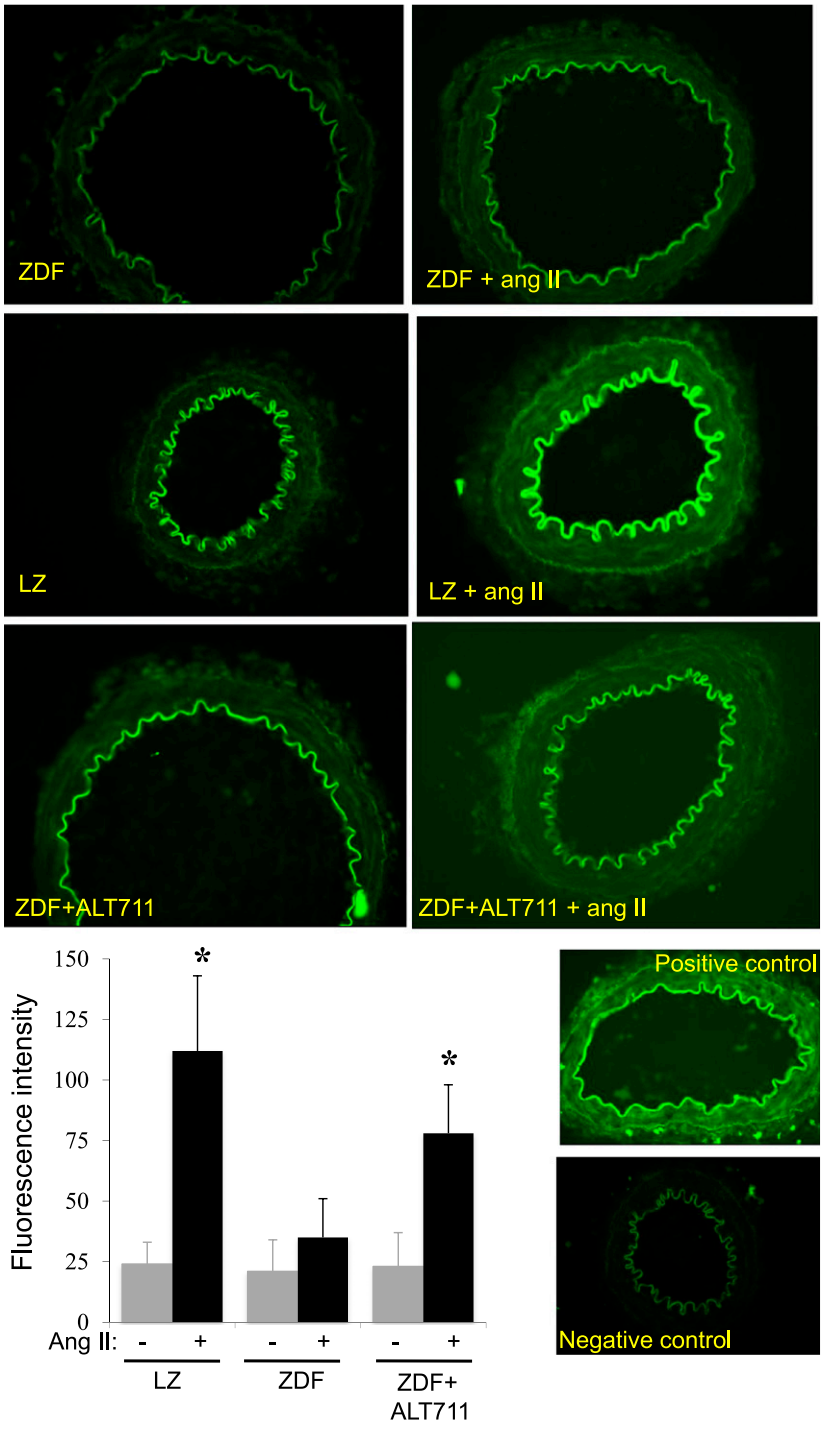

FIG. 7. Images showing in situ zymography obtained in arterial thin sections submitted to angiotensin II or not. Gelatinase activity was visualized as an enhanced fluorescence of a fluorogenic gelatin substrate in NF and HF arteries using confocal microscopy. *Bar graph*: Quantification of gelatinolytic activity was performed using image density analysis (three to four arterial sections per artery and six rats per group). Means ± SEM are presented. *$P < 0.05$, angiotensin II vs. control. (A high-quality color representation of this figure is available in the online issue.)

ACKNOWLEDGMENTS

This work was supported in part by the Foundation for Medical Research (Fondation pour la Recherche Médicale, FRM), Paris, France. M.L.F. was supported by a grant from Intervet/Schering-Plough, Angers, France.

No potential conflicts of interest relevant to this article were reported.

M.L.F. wrote the manuscript and researched data. K.T. and B.T. researched data. C.F. and L.L. contributed to the discussion and reviewed and edited the manuscript. D.H. designed the protocol, obtained grants, and wrote the manuscript. D.H. is the guarantor of this work and, as such, had full access to all the data in the study and takes responsibility for the integrity of the data and the accuracy of the data analysis.

The authors thank Jérôme Roux, Pierre Legras, and Dominique Gilbert (Animal Care Facility, University of Angers) for their kind help in treating the rats.

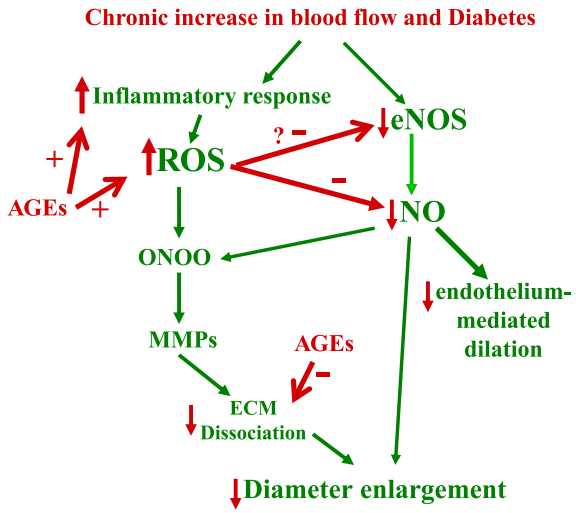

FIG. 8. Flow-mediated outward remodeling in a rat model of type 2 diabetes. A chronic increase in blood flow induces inflammation and oxidative stress. ROS associated with NO form peroxinitrite (ONOO), which activate MMPs and extracellular matrix (ECM) digestion. NO produced by eNOS after stimulation by flow (shear stress) then is able to induce diameter enlargement. In type 2 diabetes, AGE formation increases ROS formation, which reduces NO-dependent dilation. AGEs also decrease MMP activity in ZDF rats. Consequently, diameter enlargement does not occur. Green arrows refer to the pathway induced in flow-mediated outward remodeling, and red arrows point out the possible deleterious effect of AGEs. (A high-quality color representation of this figure is available in the online issue.)

REFERENCES

1. Wild S, Roglic G, Green A, Sicree R, King H. Global prevalence of diabetes: estimates for the year 2000 and projections for 2030. Diabetes Care 2004; 27:1047–1053
2. Goldstein BJ. Insulin resistance as the core defect in type 2 diabetes mellitus. Am J Cardiol 2002;90(5A):3G–10G
3. Wilson PW, D'Agostino RB, Parise H, Sullivan L, Meigs JB. Metabolic syndrome as a precursor of cardiovascular disease and type 2 diabetes mellitus. Circulation 2005;112:3066–3072
4. Pieper GM, Siebeneich W. Diabetes-induced endothelial dysfunction is prevented by long-term treatment with the modified iron chelator, hydroxyethyl starch conjugated-deferoxamine. J Cardiovasc Pharmacol 1997;30:734–738
5. Winer N, Sowers JR. Diabetes and arterial stiffening. Adv Cardiol 2007;44: 245–251
6. Belin de Chantemèle EJ, Vessières E, Guihot AL, et al. Type 2 diabetes severely impairs structural and functional adaptation of rat resistance arteries to chronic changes in blood flow. Cardiovasc Res 2009;81:788–796
7. Pourageaud F, De Mey JG. Vasomotor responses in chronically hyperperfused and hypoperfused rat mesenteric arteries. Am J Physiol 1998;274: H1301–H1307
8. Tulis DA, Unthank JL, Prewitt RL. Flow-induced arterial remodeling in rat mesenteric vasculature. Am J Physiol 1998;274:H874–H882
9. Bouvet C, Belin de Chantemèle E, Guihot AL, et al. Flow-induced remodeling in resistance arteries from obese Zucker rats is associated with endothelial dysfunction. Hypertension 2007;50:248–254
10. van den Akker J, Schoorl MJ, Bakker EN, Vanbavel E. Small artery remodeling: current concepts and questions. J Vasc Res 2010;47:183–202
11. Tronc F, Wassef M, Esposito B, Henrion D, Glagov S, Tedgui A. Role of NO in flow-induced remodeling of the rabbit common carotid artery. Arterioscler Thromb Vasc Biol 1996;16:1256–1262
12. Yan C, Huang A, Kaley G, Sun D. Chronic high blood flow potentiates shear stress-induced release of NO in arteries of aged rats. Am J Physiol Heart Circ Physiol 2007;293:H3105–H3110
13. Wautier JL, Wautier MP, Schmidt AM, et al. Advanced glycation end products (AGEs) on the surface of diabetic erythrocytes bind to the vessel wall via a specific receptor inducing oxidant stress in the vasculature: a link between surface-associated AGEs and diabetic complications. Proc Natl Acad Sci USA 1994;91:7742–7746
14. Portik-Dobos V, Anstadt MP, Hutchinson J, Bannan M, Ergul A. Evidence for a matrix metalloproteinase induction/activation system in arterial vasculature and decreased synthesis and activity in diabetes. Diabetes 2002;51:3063–3068
15. Castier Y, Brandes RP, Leseche G, Tedgui A, Lehoux S. p47phox-dependent NADPH oxidase regulates flow-induced vascular remodeling. Circ Res 2005; 97:533–540
16. Ulrich P, Cerami A. Protein glycation, diabetes, and aging. Recent Prog Horm Res 2001;56:1–21
17. Su J, Lucchesi PA, Gonzalez-Villalobos RA, et al. Role of advanced glycation end products with oxidative stress in resistance artery dysfunction in type 2 diabetic mice. Arterioscler Thromb Vasc Biol 2008;28:1432–1438
18. Loufrani L, Levy BI, Henrion D. Defect in microvascular adaptation to chronic changes in blood flow in mice lacking the gene encoding for dystrophin. Circ Res 2002;91:1183–1189
19. Pourageaud F, De Mey JG. Structural properties of rat mesenteric small arteries after 4-wk exposure to elevated or reduced blood flow. Am J Physiol 1997;273:H1699–H1706
20. Tuttle JL, Nachreiner RD, Bhuller AS, et al. Shear level influences resistance artery remodeling: wall dimensions, cell density, and eNOS expression. Am J Physiol Heart Circ Physiol 2001;281:H1380–H1389
21. Unthank JL, Nixon JC, Burkhart HM, Fath SW, Dalsing MC. Early collateral and microvascular adaptations to intestinal artery occlusion in rat. Am J Physiol 1996;271:H914–H923
22. Dumont O, Pinaud F, Guihot AL, Baufreton C, Loufrani L, Henrion D. Alteration in flow (shear stress)-induced remodelling in rat resistance arteries with aging: improvement by a treatment with hydralazine. Cardiovasc Res 2008;77:600–608
23. Driss AB, Devaux C, Henrion D, et al. Hemodynamic stresses induce endothelial dysfunction and remodeling of pulmonary artery in experimental compensated heart failure. Circulation 2000;101:2764–2770
24. Retailleau K, Belin de Chantemèle EJ, Chanoine S, et al. Reactive oxygen species and cyclooxygenase 2-derived thromboxane A2 reduce angiotensin II type 2 receptor vasorelaxation in diabetic rat resistance arteries. Hypertension 2010;55:339–344
25. Belin de Chantemèle EJ, Retailleau K, Pinaud F, et al. Notch3 is a major regulator of vascular tone in cerebral and tail resistance arteries. Arterioscler Thromb Vasc Biol 2008;28:2216–2224
26. Henrion D, Laher I, Laporte R, Bevan JA. Further evidence from an elastic artery that angiotensin II amplifies noradrenaline-induced contraction through activation of protein kinase C. Eur J Pharmacol 1992;224:13–20
27. Dowell FJ, Henrion D, Benessiano J, Poitevin P, Levy B. Chronic infusion of low-dose angiotensin II potentiates the adrenergic response in vivo. J Hypertens 1996;14:177–182
28. Vessières E, Belin de Chantemèle EJ, Toutain B, et al. Cyclooxygenase-2 inhibition restored endothelium-mediated relaxation in old obese Zucker rat mesenteric arteries. Front Physiol 2010;1:145
29. Tamarat R, Silvestre JS, Huijberts M, et al. Blockade of advanced glycation end-product formation restores ischemia-induced angiogenesis in diabetic mice. Proc Natl Acad Sci USA 2003;100:8555–8560
30. Brouwers O, Niessen PM, Haenen G, et al. Hyperglycaemia-induced impairment of endothelium-dependent vasorelaxation in rat mesenteric arteries is mediated by intracellular methylglyoxal levels in a pathway dependent on oxidative stress. Diabetologia 2010;53:989–1000
31. Dumont O, Loufrani L, Henrion D. Key role of the NO-pathway and matrix metalloprotease-9 in high blood flow-induced remodeling of rat resistance arteries. Arterioscler Thromb Vasc Biol 2007;27:317–324
32. Belin de Chantemèle EJ, Vessières E, Dumont O, et al. Reactive oxygen species are necessary for high flow (shear stress)-induced diameter enlargement of rat resistance arteries. Microcirculation 2009;16:391–402
33. Walter A, Etienne-Selloum N, Sarr M, Kane MO, Beretz A, Schini-Kerth VB. Angiotensin II induces the vascular expression of VEGF and MMP-2 in vivo: preventive effect of red wine polyphenols. J Vasc Res 2008;45:386–394
34. Loufrani L, Li Z, Lévy BI, Paulin D, Henrion D. Excessive microvascular adaptation to changes in blood flow in mice lacking gene encoding for desmin. Arterioscler Thromb Vasc Biol 2002;22:1579–1584
35. Eichmann A, Yuan L, Moyon D, Lenoble F, Pardanaud L, Breant C. Vascular development: from precursor cells to branched arterial and venous networks. Int J Dev Biol 2005;49:259–267
36. Hilgers RH, Schiffers PM, Aartsen WM, Fazzi GE, Smits JF, De Mey JG. Tissue angiotensin-converting enzyme in imposed and physiological flow-related arterial remodeling in mice. Arterioscler Thromb Vasc Biol 2004;24: 892–897
37. Kojda G, Hambrecht R. Molecular mechanisms of vascular adaptations to exercise: physical activity as an effective antioxidant therapy? Cardiovasc Res 2005;67:187–197
38. Gorny D, Loufrani L, Kubis N, Lévy BI, Henrion D. Chronic hydralazine improves flow (shear stress)-induced endothelium-dependent dilation in mouse mesenteric resistance arteries in vitro. Microvasc Res 2002;64:127–134

39. Sorop O, Bakker EN, Pistea A, Spaan JA, VanBavel E. Calcium channel blockade prevents pressure-dependent inward remodeling in isolated subendocardial resistance vessels. Am J Physiol Heart Circ Physiol 2006; 291:H1236–H1245
40. Heil M, Ziegelhoeffer T, Wagner S, et al. Collateral artery growth (arteriogenesis) after experimental arterial occlusion is impaired in mice lacking CC-chemokine receptor-2. Circ Res 2004;94:671–677
41. Steinberg HO, Chaker H, Leaming R, Johnson A, Brechtel G, Baron AD. Obesity/insulin resistance is associated with endothelial dysfunction: implications for the syndrome of insulin resistance. J Clin Invest 1996;97: 2601–2610
42. Endemann DH, Pu Q, De Ciuceis C, et al. Persistent remodeling of resistance arteries in type 2 diabetic patients on antihypertensive treatment. Hypertension 2004;43:399–404
43. Crijns FR, Wolffenbuttel BH, De Mey JG, Struijker Boudier HA. Mechanical properties of mesenteric arteries in diabetic rats: consequences of outward remodeling. Am J Physiol 1999;276:H1672–H1677
44. Cooper ME, Rumble J, Komers R, Du HC, Jandeleit K, Chou ST. Diabetes-associated mesenteric vascular hypertrophy is attenuated by angiotensin-converting enzyme inhibition. Diabetes 1994;43:1221–1228
45. Rumble JR, Cooper ME, Soulis T, et al. Vascular hypertrophy in experimental diabetes: role of advanced glycation end products. J Clin Invest 1997;99:1016–1027
46. Goldin A, Beckman JA, Schmidt AM, Creager MA. Advanced glycation end products: sparking the development of diabetic vascular injury. Circulation 2006;114:597–605
47. Stirban A, Negrean M, Stratmann B, et al. Benfotiamine prevents macro- and microvascular endothelial dysfunction and oxidative stress following a meal rich in advanced glycation end products in individuals with type 2 diabetes. Diabetes Care 2006;29:2064–2071
48. Sun D, Huang A, Koller A, Kaley G. Decreased arteriolar sensitivity to shear stress in adult rats is reversed by chronic exercise activity. Microcirculation 2002;9:91–97